HHS Public Access

Author manuscript

Biomaterials. Author manuscript; available in PMC 2019 September 01.

Published in final edited form as:

Biomaterials. 2018 September ; 178: 293–301. doi:10.1016/j.biomaterials.2018.06.025.

A Paradigm of Endothelium-Protective and Stent-Free Anti-Restenotic Therapy Using Biomimetic Nanoclusters

Bowen Wang[1,#], **Guojun Chen**[2,#], **Go Urabe**[1], **Ruosen Xie**[2], **Yuyuan Wang**[2], **Xudong Shi**[3], **Lian-Wang Guo**[4,*], **Shaoqin Gong**[2,5,*], and **K. Craig Kent**[1,*]

[1]Department of Surgery, College of Medicine, the Ohio State University, Columbus, OH 43210, USA

[2]Department of Materials Science and Engineering, and Wisconsin Institute for Discovery, University of Wisconsin-Madison, Madison, WI 53715, USA

[3]Department of Surgery, 5151 Wisconsin Institute for Medical Research, University of Wisconsin-Madison, 1111 Highland Ave, Madison, WI 53705, USA

[4]Department of Surgery, Department of Physiology & Cell Biology, Davis Heart and Lung Research Institute, the Ohio State University, Columbus, OH 43210, USA

[5]Department of Biomedical Engineering and Department of Chemistry, University of Wisconsin-Madison, Madison, WI 53715, USA

Abstract

Drug-eluting stents are the most commonly employed method to control post-angioplasty restenosis. Unfortunately, they exacerbate life-threatening stent thrombosis because of endothelium damage caused by both drug and stenting. To solve this major medical problem, an endothelium-protective and stent-free anti-restenotic method is highly desirable. Here we have generated a biomimetic intravenous delivery system using dendritic polymer-based nanoclusters, which were coated with platelet membranes for targeting to the injured arterial wall where restenosis occurs. These nanoclusters were loaded with an endothelium-protective epigenetic inhibitor (JQ1) or an endothelium-toxic status quo drug (rapamycin), and compared for their ability to mitigate restenosis without hindering the process of re-endothelialization. Fluorescence imaging of Cy5-tagged biomimetic nanoclusters indicated their robust homing to injured, but not uninjured arteries. Two weeks after angioplasty, compared to no-drug control, both rapamycin- and JQ1-loaded biomimetic nanoclusters substantially reduced (by >60%) neointimal hyperplasia,

[*]Corresponding authors: K. Craig Kent, M.D. KC.Kent@osumc.edu. Shaoqin Gong, Ph.D. shaoqingong@wisc.edu. Lian-Wang Guo, Ph.D. Lianwang.Guo@osumc.edu.

[#]These authors contributed equally to this work.

Author contributions: B.W., G.C., L.-W.G., S.G., and K.C.K. designed the studies; B.W., G.C., G.U., Y.W., and X.S. performed experiments; B.W., G.C., L.-W.G., and S.G. wrote the manuscript; B.W., G.C., L.-W.G., S.G., and K.C.K. critically reviewed the manuscript.

Disclosures: The authors declare no conflicts of interest.

the primary cause of restenosis. However, whereas the rapamycin formulation impaired the endothelial re-coverage of the denuded inner arterial wall, the JQ1 formulation preserved endothelial recovery. In summary, we have created an endothelium-protective anti-restenotic system with biomimetic nanoclusters containing an epigenetic inhibitor. This system warrants further development for a non-thrombogenic and stent-free method for clinical applications.

Keywords

Biomimetic nanoclusters; endothelium-protective; JQ1; rapamycin; re-endothelialization

1. Introduction

Drug-eluting stents (DES) represent a major medical advance in reducing restenosis, the re-blockage of angioplastied atherosclerotic arteries. However, stent thrombosis has become a major concern[1]. The problem is two-fold. First, implanting a stent, a foreign object, is pro-inflammatory and thrombogenic, and also triggers neointimal hyperplasia (IH), the chief etiology of restenosis. Second, the anti-proliferative drugs coated on stents to curb IH including paclitaxel and rapamycin also block endothelial cell (EC) re-growth (termed re-endothelialization), thereby exacerbating stent thrombogenicity[2]. The most adverse consequence of stent thrombosis is high rates (up to 50%) of death even though the incidence of stent thrombosis is no more than 1.5% [1]. Anti-coagulant therapies cannot completely prevent stent thrombosis, and they are associated with high costs and bleeding problems. Aside from all of these complications, compromised DES cannot be replaced, and hence a secondary, invasive revascularization such as bypass surgery is often required[1]. Therefore, there is a clear clinical need for the development of an endothelium-protective and stent-free anti-restenotic therapy via innovations in both drug and its delivery method.

The recent discovery of small molecule inhibitors (JQ1 as the first in class)[3] that selectively block the bromo and extraterminal (BET) domain family of epigenetic reader proteins has opened the door to effectively treating previously recalcitrant condition[4]. These inhibitors have shown excellent efficacy in treating proliferative and inflammatory diseases, such as cancer and heart failure, in preclinical tests or clinical trials[4]. Of particular interest, our study using a rat model showed that JQ1 is an effective inhibitor of restenosis[5]. More significantly, JQ1 also exhibited a prominent EC-protective effect in vitro and in vivo[5, 6], which is a rare feature among the numerous anti-restenotic agents[7]. Moreover, rapidly growing evidence supports a mechanism whereby JQ1 disrupts molecular complexes formed by BET proteins, transcription factors, super enhancers and/or other regulators that cooperatively define BET protein functional specificity[4]. As such, JQ1 and its analogs appear to be promising EC-protective candidate drugs suitable for next-generation anti-restenotic therapy.

To administer JQ1 in a non-invasive stent-free fashion, targeted intravenous delivery to the injured arterial wall should be the preferable method. Both nanoparticle (NP)-based and cell-based approaches have been extensively explored for targeted delivery[8]. While systemically delivered “alien” NPs can elicit inflammatory responses, effects of cell therapy

also are complicated by immune reactions. To reconcile the benefits and drawbacks of these two approaches, biomembrane-coated PLGA NPs have emerged as a novel biomimetic platform for delivery of therapeutics[9]. They have shown excellent homing to injured tissues and minimal immunogenicity in that proof-of-concept study.

In the current study, we applied this biomimicry/nanotechnology hybrid concept in a rat model of balloon angioplasty for targeted intravenous delivery of JQ1, an endothelium-protective BET inhibitor[5, 6], in comparison to rapamycin, a status quo drug known to be EC-toxic[2, 7]. JQ1 or rapamycin was loaded into nanoclusters formed by multiple PAMAM-polyvalerolactone (PAMAM-PVL) ultrasmall unimolecular NPs. These nanoclusters were then coated with platelet membranes that were deprived of immunogenicity[9] yet retaining the ability to target injured tissues, hereby termed biomimetic nanoclusters. We observed their robust homing to balloon-injured areas in arteries. Remarkably, whereas rapamycin/nanoclusters inhibited IH as well as re-endothelialization, JQ1/nanoclusters preserved the ability of the endothelium to recover while mitigating IH.

2. Materials and Methods

2.1 Ethics statement

All animal studies conform to the Guide for the Care and Use of Laboratory Animals (National Institutes of Health) and protocols approved by the Institutional Animal Care and Use Committees at the University of Wisconsin and The Ohio State University. Institutional review board (IRB) approval has been obtained for use of human samples.

2.2 Reagents and materials

Human platelets and platelet membranes were purchased from Zen-Bio Inc (Research Triangle Park, NC). RNAlater solution, TRIzol, SuperScript IV VILO Master Mix, and SYBR Green PCR Mastermix was purchased from Thermo Fisher Scientific (Waltham, MA). Poly(amidoamine) (PAMAM; 4th generation dendrimer), Evans Blue, dimethyl sulfoxide (DMSO), valerolactone (VL), and stannous (II) octoate ($Sn(Oct)_2$) were purchased from Sigma-Aldrich (St. Louis, MO). Rapamycin was purchased from LC Laboratories (Woburn, MA). JQ1 was purchased from ApexBio (Houston, TX). Cy5 dye was obtained from Lumiprobe Co. (Hallandale Beach, FL). Reagents not otherwise specified were purchased from Thermo Fisher Scientific (Fitchburg, WI).

2.3 Synthesis of drug-loaded biomimetic nanoclusters

(a). Synthesis of Cy5-tagged ultrasmall unimolecular NPs (PAMAM-PVL-COOH/Cy5)—PAMAM-PVL-OH was first prepared by ring-opening polymerization as reported previously[10]. Thereafter, PAMAM-PVL-OH (50 mg) was reacted with succinic anhydride (8.2 mg) in the presence of 4-dimethylaminopyridine (12.5 mg) to yield PAMAM-PVL-COOH. The PAMAM-PVL-COOH/Cy5 was prepared by the reaction between PAMAM-PVL-COOH and Cy5-NH_2. Briefly, PAMAM-PVL-COOH (20 mg), N-hydroxysuccinimide (0.9 mg), and dicyclohexylcarbodiimide (2.1 mg) were added into dimethylformamide (5 mL). The solution was stirred for 30 min at 0°C. Thereafter, Cy5 (3.1

mg) was added into the solution. The reaction was carried out in the dark overnight. The impurities were then removed by dialysis against DI water for 48 h. The final product was dried under lyophilization.

(b). Synthesis of drug-loaded PAMAM-PVL ultrasmall unimolecular NPs— PAMAM-PVL-COOH (50 mg) and JQ1 (20 mg) were dissolved in DMSO (5 mL). DI water (15 mL) was added dropwise into the above solution over 30 min. Thereafter, the unloaded drugs and DMSO were removed by dialysis against DI water for 48 h. The JQ1-loaded NPs were obtained after lyophilization. The rapamycin-loaded ultrasmall unimolecular NPs were prepared following a similar method.

(c). Synthesis of drug-loaded biomimetic nanoclusters—The platelet membrane was derived as previously reported[9]. Biomimetic nanoclusters were prepared by dispersing and fusing platelet membrane vesicles with PAMAM-PVL-COOH or PAMMA-PVL-COOH/Cy5 under sonication for 2 min (100 μg of PAMAM to 20 μl of platelet vesicle solution). The drug-loaded nanoclusters were prepared following a similar protocol by fusing drug-loaded (i.e., rapamycin and JQ1) ultrasmall unimolecular NPs with platelet membranes.

(d). Characterizations—^{1}H NMR spectra of all polymer products were recorded on a Varian Mercury Plus 300 spectrometer in DMSO–d_6 or $CDCl_3$ at 25 °C. Molecular weights (M_n and M_w) and polydispersity indices (PDI) of the polymers were determined by a gel permeation chromatographer (GPC) equipped with a refractive index detector, a viscometer detector, and a light scattering detector (Viscotek, USA). DMF with 0.01 M of LiBr was used as the mobile phase with. Fourier transform infrared (FT-IR) spectra were recorded on a Bruker Tensor 27 FT-IR spectrometer. The sizes and morphologies of the NPs were studied by dynamic light scattering (DLS, ZetaSizer Nano ZS90, Malvern Instruments, USA) and transmission electron microscopy (TEM, FEI Tecnai G^2 F30 TWIN 300 KV, E.A. Fischione Instruments, Inc. USA). The zeta potentials were measured by ZetaSizer Nano ZS90 (Malvern Instruments, USA). The rapamycin loading level was measured by high-performance liquid chromatography (HPLC) using ultraviolet (UV) detection at 278 nm. The JQ1 loading level was measured by UV-Vis spectrometer at 323 nm.

2.4 In vitro drug release

The *in* vitro drug release profiles from both rapamycin-loaded and JQ1-loaded biomimetic nanoclusters were studied in PBS (pH = 7.4)[11]. Briefly, drug-loaded biomimetic nanoclusters in the PBS (1 mg/mL, 5 mL) were enclosed in a cellulose membrane dialysis bag (molecular weight cut–off, 8 kDa). The dialysis bags were immersed in 100 mL of PBS, which was then kept in a horizontal laboratory shaker (100 rpm) at 37°C. At predetermined time intervals, 5 mL samples were collected and replaced with the same volume of PBS. The amounts of rapamycin and JQ1 in the collected samples were measured by HPLC and UV-Vis spectrometer, respectively, as indicated above.

2.5 Rat carotid artery balloon angioplasty

Carotid artery balloon angioplasty was performed in male Sprague–Dawley rats (Charles River; ~400 g) as previously described[5, 12]. Briefly, rats were anesthetized with isoflurane (5% for inducing and 2.5% for maintaining anesthesia). A longitudinal incision was made in the neck and carotid arteries were exposed. A 2-F balloon catheter (Edwards Lifesciences, Irvine, CA) was inserted through an arteriotomy on the left external carotid artery. To produce arterial injury, the balloon was inflated at a pressure of 2 atm and withdrawn to the carotid bifurcation and this action was repeated three times. The external carotid artery was then permanently ligated, and blood flow was resumed. Drug-loaded biomimetic nanoclusters or compound solutions were injected via rat tail vein. Animals were euthanized in a CO_2 chamber at day 5 (for artery ex vivo imaging) or day 14 (for morphometric analysis) after balloon injury.

2.6 IVIS imaging for homing of biomimetic nanoclusters

Cy5-tagged nanoclusters were coated with platelet membranes, as described above, and tail-vein injected (2.5 mg/kg animal weight) immediately after balloon angioplasty of the rat carotid artery. Animal were euthanized 5 days later. Various organs (see Figure S1) including balloon-Injured arteries and uninjured contralateral arteries were collected. Ex vivo fluorescence imaging was performed to track Cy5-tagged nanoclusters using an IVIS spectrum luminescence system (Ex/Em: 650/720 nm).

2.7 Morphometric analysis of neointima

Two weeks after balloon angioplasty, common carotid arteries were collected from anesthetized animals (under 2.5% isoflurane) following perfusion fixation at a physiological pressure of 100 mm Hg. The animals were then euthanized. Paraffin sections (5 μm thick) were excised from carotid arteries at equally spaced intervals and then Van Gieson stained for morphometric analysis, as described in our previous reports[5, 12]. Planimetric parameters as follows were measured on the sections and calculated using Image J: area inside external elastic lamina (EEL area), area inside internal elastic lamina (IEL area), lumen area, intima area (= IEL area – lumen area), and media area (= EEL area – IEL area). Intimal hyperplasia was quantified as a ratio of intima area versus media area. Measurements were performed by a researcher blinded to the experimental conditions using 3–6 sections from each of animal. The data from all sections were pooled to generate the mean for each animal. The means from all the animals in each treatment group were then averaged, and the standard error of the mean (SEM) was calculated.

2.8 Re-endothelialization study with Evans Blue dye

Re-endothelialization in balloon-injured arteries was evaluated on day 5 after angioplasty using Evans Blue assay according to the previously published method with minor modifications[12]. Briefly, 1 ml of 0.5% Evans Blue dye was injected into tail vein under anesthesia by 2.5% isoflurane. After 30 min, rats were perfused with 10 ml of PBS buffer, followed by 10 ml perfusion with RNAlater to transiently preserve RNA in endothelium. The common carotid arteries were dissected and peri-adventitial connective tissues were trimmed to avoid contamination in downstream RNA extraction. Common carotid arteries

were collected starting from the proximal end to the aortic arch, and were then longitudinally opened and photographed on a white background. Denuded areas were stained blue; unstained areas indicate re-endothelialization and were quantified using Image J. For the calculation of re-endothelialization index refer to Figure 3 legend.

Immediately after images were taken, the carotid segments were rinsed in PBS multiple times, dried on Kimwipes, and snap-frozen in liquid nitrogen, until later processed for tissue RNA extraction.

2.9 Real-time Quantitative PCR (qRT-PCR)

mRNA was isolated from collected carotid segments using TRIzol following the manufacturer's instructions. Purified mRNA (1 μg) was used for the first-strand cDNA synthesis and quantitative RT-PCR was performed using the 7500 Fast Real-Time PCR System (Applied Biosystems, Carlsbad, CA). Each cDNA template was amplified in triplicates using SYBR Green PCR Master Mix, with the following primer sets: Rat VCAM1 forward primer CTCCTCTCGGGAAATGCCAC, reverse primer AACAACGGAATCCCCAACCT; Rat MCP1 forward primer CTTCCAAGTGGCTAAGGGCA, reverse primer TCAAAGGGAGTCGGGGATCT; Rat Flk1 forward primer CTTCCAAGTGGCTAAGGGCA, reverse primer TCAAAGGGAGTCGGGGATCT; Rat GAPDH forward primer GACATGCCGCCTGGAGAAAC, reverse primer AGCCCAGGATGCCCTTTAGT.

2.10 Statistical Analysis

Data are presented as mean ± standard error of the mean (SEM). Statistical analysis was conducted using one-way ANOVA followed by Bonferroni post-hoc tests. Data are considered statistically significant when a P value is at least < 0.05.

3. Results

3.1 Biomimetic nanoclusters effectively home to the balloon-injured carotid artery wall

Biomimetic (platelet membrane-coated) nanoclusters were prepared as indicated in Figure 1. Detailed characterization of the biomimetic nanoclusters (e.g., size, zeta potential, and drug release profiles) can be found in the supplemental file (Table S1 and Figure S2). Their post-injection homing was visualized via the Cy5 fluorophores that were conjugated to the unimolecular NPs forming the nanoclusters. Immediately after balloon angioplasty in the rat carotid artery, biomimetic nanoclusters (2.5 mg/kg) which were readily dispersible, were injected into the tail vein. Five days later, arteries were collected for ex vivo Cy5 imaging using an in vivo imaging system (IVIS). We observed strong Cy5 fluorescent signals in injured artery segments, but could not detect Cy5 signals in the uninjured contralateral artery (Figure 2 and Figure S3). The imaging data suggest that systemically delivered platelet-membrane-coated nanoclusters can effectively target, and then accumulate on the injured arterial wall.

3.2 JQ1-loaded but not rapamycin-loaded biomimetic nanoclusters preserve re-endothelialization of injured arteries

The major objective of this study was to create an endothelium-protective anti-restenotic system employing drug-containing biomimetic nanoclusters. We therefore compared the impacts of the rapamycin- and JQ1-containing nanocluster formulations on re-endothelialization 5 days after angioplasty (Figure 3). Since the nanoclusters without platelet membrane coating were prone to form aggregates, which prevented injection, we did not include this condition in the experiments. As revealed in Figure 3A, right after angioplasty, the inner surface of balloon-injured artery was almost fully stained by Evans Blue, indicating denudation of endothelium. After 5 days without treatment, the proximal end of the injured artery could no longer be stained, indicative of re-coverage of this area by newly grown ECs. Consistent with a known EC-toxic effect[2], rapamycin delivered in biomimetic nanoclusters substantially impaired re-endothelialization. Remarkably, we found that this detrimental effect did not occur in the arteries treated with JQ1-loaded biomimetic nanoclusters. Rather, the treated arteries had even a greater endothelial coverage than empty nanoclusters (no drug), although the increase did not reach statistical significance in this experimental setting (Figure 3B). Re-endothelialization progressed mainly from the proximal side of the denuded artery likely because at the distal end it was too slow to observe, which is common with the balloon angioplasty model[13]. To further confirm this endothelium-preserving effect of the JQ1/nanocluster formulation, we determined its influence on EC phenotypic markers. Indeed, compared to control (vehicle, no drug), whereas the rapamycin/nanocluster formulation markedly increased the expression of VCAM-1 and MCP-1 mRNA, both markers of EC dysfunction or deterioration[14–17], the JQ1/nanocluster formulation did not increase the expression of these two markers (Figure 3C). Consistently, JQ1/nanoclusters did not, but rapamycin/nanoclusters did reduce the expression of Flk-1, a vascular endothelial growth factor receptor and a well-established EC marker[18]. The eNOS level is an endothelial functional indicator[19]. Whereas JQ1/nanoclusters elevated eNOS mRNA up to three-fold, rapamycin/nanoclusters did not produce a significant effect (Figure S4).

3.3 JQ1-loaded biomimetic nanoclusters effectively inhibit the development of neointima

We then compared the anti-restenotic effects of biomimetic nanoclusters loaded with rapamycin and JQ1, respectively. These drug-loaded biomimetic nanoclusters, or their respective drug-only controls (no nanoclusters), were intravenously injected immediately after balloon angioplasty. The injections were repeated 4 days later. In parallel, additional controls of PBS and empty biomimetic nanoclusters (no drug) were injected. The doses of rapamycin (0.25 mg/kg/injection) and JQ1 (5 mg/kg/injection) were chosen based on previous publications[2, 5] and our pilot experiments (data not shown). Two weeks after angioplasty, carotid arteries were collected for morphometric analysis. As shown in Figure 4, compared to vehicle-only control, empty biomimetic nanoclusters did not affect IH (measured by the I/M ratio). Compared to these two controls or drug-only controls (no nanoclusters), both rapamycin- and JQ1-loaded biomimetic nanoclusters inhibited IH by >60% (Figure 4C) with the overall vessel size unaltered (Figure S5). Although both formulations increased the lumen size, the effect of JQ1-loaded nanoclusters appeared to be more prominent. Interestingly, intravenous delivery of the same dose of free rapamycin or

free JQ1 without using nanoclusters failed to mitigate IH. This indicates that delivery of rapamycin or JQ1 in a targeted manner using biomimetic nanoclusters can reduce the dose required for effective attenuation of IH. The JQ1/nanoclusters did not lead to systemic toxicity, as evidenced from the normal tissue morphologies of rat brain, heart, kidney, liver, and spleen (Figure S6) and the lack of increase of inflammatory cytokines in spleen and liver tissues (Figure S7). This is consistent with the lack of cell toxicity of membrane-coated nanoclusters (Figures S8 and S9). Moreover, similar to the control rats injected with vehicle/nanoclusters, the animals injected with JQ1/nanoclusters showed a 10% increase of body weight in ten days (Day 4 to Day 14 post angioplasty), suggesting that the JQ1/nanoclusters did not disrupt the animals' natural weight gain during growth (Figure S10). However, the rapamycin/nanoclusters caused ~6% decrease of body weight within these ten days. This acute weight loss possibly reflects a toxic effect. Toxicity of systemically circulated rapamycin has been previously reported[20–22].

4. Discussion

DES implantation has become a procedure prevailingly used in the clinic to control post-angioplasty restenosis in the treatment of atherosclerosis. Unfortunately, it has been widely reported that DES exacerbates life-threatening stent thrombosis[1]. This adverse effect is believed to stem from both the EC-toxic drug (e.g., rapamycin) coated on the stent and the stent itself as a non-biological object that intrudes into vascular tissues[1, 2]. Here we have created a prototype stent-free biomimetic system that not only mitigates IH but importantly, also protects re-endothelialization, the healing step most critical to thrombosis prevention. This biomimetic formulation incorporates multiple innovations. First, it is injectable and hence stent-free. Second, the nanocluster is a more advanced drug nanocarrier than traditional NPs. Third, coating with biomembranes enables homing of drug-containing nanoclusters to the injury site where IH and thrombosis occur. Lastly, yet importantly, JQ1 represents a novel anti-restenotic epigenetic modulator with a unique function of endothelial protection[5, 6, 23]. These features (further discussed below) together outline a new paradigm for a non-thrombogenic and stent-free anti-restenotic therapy.

Aside from a thrombogenic risk, other drawbacks inherent to DES are prominent as well. A stent insinuated into the arterial wall inflicts not only smooth muscle cell injury but also EC damage, both synergistically contributing to neointimal proliferation[24]. Ample clinical evidence indicates that neointima can grow into the lumen through the struts of DES, causing in-stent restenosis[1]. Because the stent is not replaceable, an invasive open surgery would become necessary to bypass the restenotic artery. In contrast, repeated intravenous injections of biomimetic nanoclusters are readily convenient. Taking advantage of this feature, the treatment regimen can be adjusted based on the specific needs of individual patients. As such, a treatment plan could be designed toward precision medicine in a personalized manner.

In this study, rather than using a traditional PLGA NP[9], we opted to use a nanocluster formed by multiple PAMAM-PVL ultrasmall unimolecular NPs, which brings several advantages to the biomimetic therapeutic system. The PAMAM-PVL dendritic polymer forms a unimolecular NP consisting of only covalent bonds which can be used to

encapsulate a hydrophobic drug[10]. Furthermore, the nanocluster allows for versatile chemical modifications. Both the core (i.e., PAMAM) and arms (i.e. PVL) can be readily modified for drug release profile optimization. Meanwhile, the dendritic polymers can be easily tailored (e.g., Cy5 in this study) to achieve multifunctionality. In addition, the nanocluster size can be controlled by adjusting the process parameters during the sonication or extrusion processes. Therefore, the nanoclusters are amenable to customization for optimal combination with biomembrane coating.

Coating nanoplatforms with biomembranes for targeted delivery represents a major innovation in nanomedicine[8]. Biomembranes serve as an interface between cells and their surrounding and mediate a myriad of interactions. They can thus be co-opted for targeting specific tissues or cells[25]. The platelet membrane coating of nanoclusters is well suited for targeting the angioplasty-injured vascular vessel wall where the sub-endothelial collagen matrix is exposed. This homing action is likely mediated by glycoprotein VI (GPVI), a physiological collagen receptor unique to the platelet cell membrane[26]. Whereas GPVI remains in the platelet membrane after membrane preparation, the cell contents essential for platelet activation are mostly depleted. As such, the platelet membrane coated on nanoclusters is still able to home to the injured arterial wall yet deprived of the signaling pathways that underlie platelet activation and aggregation[9]. Indeed, we did not observe thrombosis in the animals injected with platelet membrane-coated nanoclusters. Along this line, we speculate that injecting platelet membrane-coated nanoclusters prior to angioplasty may confer a temporal edge for them to occupy the injury site while warding off native platelets. It takes future experiments to test the therapeutic benefits of this approach.

A prominent benefit of targeted delivery is a drastic decrease in effective drug doses. For example, the total amount of JQ1 used in our biomimetic nanoclusters (two injections) is ~70 fold lower than the combined free JQ1 (twice daily injections) used for systemic delivery[3]. This can be rationalized by reduced drug clearance rate, protection of drug by nanoclusters, and relatively high local drug concentrations at targeted sites. Lower effective JQ1 dose achieved using biomimetic nanoclusters should reduce side-effect concerns. While JQ1 is generally deemed nontoxic[27], it possibly blocks memory[28] or restrains bone growth in animals[29], underscoring the necessity of targeted delivery. It is worth noting that we did not observe obvious inflammatory responses resulting from the coated nanoclusters, either in animal tissues (Figure S7) or in cultured smooth muscle or endothelial cells (Figures S8 and S9). This is likely because the platelets were pre-inactivated with prostaglandin E1 and the platelet activation signaling machinery was sabotaged during membrane preparation [9]. In contrast, non-coated nanoclusters incited cell apoptosis and impaired cell viability (Figures S8 and S9), likely due to their tendency to aggregate. In addition, in our study platelet membrane coating renders drug-loaded nanoclusters readily dispersible in aqueous solutions and injectable. It is otherwise not practical to inject the non-coated nanoclusters as they are prone to form large aggregates, likely due to the relatively hydrophobic nature of the nanoclusters, which in fact is desirable for the platelet-membrane coating process.

A unique feature of our anti-restenotic biomimetic system is its endothelium-protective effect, which is largely owing to JQ1. In a stark contrast, the rapamycin/biomimetic

nanocluster formulation impairs re-endothelialization. Previous studies including our own showed that JQ1 inhibits smooth muscle cell proliferation that forms neointima yet protects EC survival[5, 6]. This may be explained by different signaling networks in the two cell types[24]. Consistently, the epigenetic functions of JQ1's target, the BET protein family, are highly cell type- and cell state-specific[4, 6]. While ECs are extremely susceptible to inflammatory insults, JQ1 proved to be a potent anti-inflammatory agent for ECs in vitro and in vivo[5, 6]. It has been recently shown that JQ1 treatment of human umbilical vein ECs inhibits TNFα-induced pathogenic EC activation which is indicated by increased expression of E-selectin and vascular cell adhesion molecule (VCAM1) and NFκB nuclear translocation[6]. Moreover, the inhibitory effects of JQ1 on pro-inflammatory activation of ECs and their monocyte recruiting were also observed in vivo in a hypercholesterolemic murine model of atherosclerosis[6]. The molecular mechanism involves BET/NFκB-orchestrated super-enhancer remodeling that mediates inflammatory transcription and cell state transition in ECs. Though highly desirable, endothelium-protective anti-restenotic agents remain scarce[7]. In this regard, identification of BET epigenetic regulators as endothelium-protective molecular targets is significant[5]. The combined strengths of EC-friendly agents such as JQ1 and stent-free, targeted delivery using biomimetic nanoclusters may open a new avenue for next-generation anti-restenotic therapy.

5. Conclusions

DES thrombogenecity is a grave concern; the key problem is impaired endothelial recovery caused by both the drugs delivered by DES and stenting[1, 2]. Developing an alternative method to DES has been a paramount challenge as it requires innovations in both drug and drug delivery device. Our site of injury-targeting biomimetic system radically departs from the status quo DES method. It has two prominent features, the use of an endothelium-protective epigenetic inhibitor and the omission of EC-damaging stenting, both contributing to the highly desirable preclinical outcome of suppressed IH and protected re-endothelialization. As endothelial damage is a common key etiology in major vascular diseases including atherosclerosis, restenosis, vein graft failure, and aneurysm[30], this anti-restenotic biomimetic system is expected to find broad applications. Though future testing is required, this system is intuitively advantageous for combination therapy, as biomembrane-coated nanoclusers containing different drugs can be mixed with varying ratios and co-injected. This confers considerable adjustability of constituent drugs, doses, and injection frequency etc., particularly in favor of personalized and precision medicine, which DES cannot provide.

Supplementary Material

Refer to Web version on PubMed Central for supplementary material.

Acknowledgments

We thank Dr. Matthew Stratton for informative discussion and proof reading.

Sources of funding: This work was supported by NIH grants R01 HL129785 (to K.C.K., S.G., and L.-W.G.), R01HL-068673 (to K.C.K.), NIH R01 HL133665 (to L.-W. G.), and EY022678 (to L.-W. G.), NIH K25CA166178 (to S.G.), and an AHA Predoctoral Award 16PRE30160010 (to B.W.).

References

1. Byrne RA, Joner M, Kastrati A. Stent thrombosis and restenosis: what have we learned and where are we going? The Andreas Gruntzig Lecture ESC 2014. European heart journal. 2015; 36(47): 3320–31. [PubMed: 26417060]
2. Camici GG, Steffel J, Amanovic I, Breitenstein A, Baldinger J, Keller S, Luscher TF, Tanner FC. Rapamycin promotes arterial thrombosis in vivo: implications for everolimus and zotarolimus eluting stents. European heart journal. 2010; 31(2):236–42. [PubMed: 19567381]
3. Filippakopoulos P, Qi J, Picaud S, Shen Y, Smith WB, Fedorov O, Morse EM, Keates T, Hickman TT, Felletar I, Philpott M, Munro S, McKeown MR, Wang Y, Christie AL, West N, Cameron MJ, Schwartz B, Heightman TD, La Thangue N, French CA, Wiest O, Kung AL, Knapp S, Bradner JE. Selective inhibition of BET bromodomains. Nature. 2010; 468(7327):1067–73. [PubMed: 20871596]
4. Wang CY, Filippakopoulos P. Beating the odds: BETs in disease. Trends in biochemical sciences. 2015; 40(8):468–79. [PubMed: 26145250]
5. Wang B, Zhang M, Takayama T, Shi X, Roenneburg DA, Kent KC, Guo LW. BET Bromodomain Blockade Mitigates Intimal Hyperplasia in Rat Carotid Arteries. EBioMedicine. 2015; 2(11):1650–61.
6. Brown JD, Lin CY, Duan Q, Griffin G, Federation AJ, Paranal RM, Bair S, Newton G, Lichtman AH, Kung AL, Yang T, Wang H, Luscinskas FW, Croce KJ, Bradner JE, Plutzky J. NF-kappaB directs dynamic super enhancer formation in inflammation and atherogenesis. Molecular cell. 2014; 56(2):219–31. [PubMed: 25263595]
7. Goel SA, Guo LW, Wang B, Guo S, Roenneburg D, Ananiev GE, Hoffmann FM, Kent KC. High-throughput screening identifies idarubicin as a preferential inhibitor of smooth muscle versus endothelial cell proliferation. PloS one. 2014; 9(2):e89349. [PubMed: 24586708]
8. Zhang P, Liu G, Chen X. Nanobiotechnology: Cell Membrane-Based Delivery Systems. Nano Today. 2017; 13:7–9. [PubMed: 28435439]
9. Hu CM, Fang RH, Wang KC, Luk BT, Thamphiwatana S, Dehaini D, Nguyen P, Angsantikul P, Wen CH, Kroll AV, Carpenter C, Ramesh M, Qu V, Patel SH, Zhu J, Shi W, Hofman FM, Chen TC, Gao W, Zhang K, Chien S, Zhang L. Nanoparticle biointerfacing by platelet membrane cloaking. Nature. 2015; 526(7571):118–21. [PubMed: 26374997]
10. Chen G, Jaskula-Sztul R, Harrison A, Dammalapati A, Xu W, Cheng Y, Chen H, Gong S. KE108-conjugated unimolecular micelles loaded with a novel HDAC inhibitor thailandepsin-A for targeted neuroendocrine cancer therapy. Biomaterials. 2016; 97:22–33. [PubMed: 27156249]
11. Zhao L, Chen G, Li J, Fu Y, Mavlyutov TA, Yao A, Nickells RW, Gong S, Guo L-W. An intraocular drug delivery system using targeted nanocarriers attenuates retinal ganglion cell degeneration. Journal of Controlled Release. 2017; 247:153–166. [PubMed: 28063892]
12. Guo LW, Wang B, Goel SA, Little C, Takayama T, Shi XD, Roenneburg D, DiRenzo D, Kent KC. Halofuginone stimulates adaptive remodeling and preserves re-endothelialization in balloon-injured rat carotid arteries. Circ Cardiovasc Interv. 2014; 7(4):594–601. [PubMed: 25074254]
13. Grassia G, Maddaluno M, Guglielmotti A, Mangano G, Biondi G, Maffia P, Ialenti A. The anti-inflammatory agent bindarit inhibits neointima formation in both rats and hyperlipidaemic mice. Cardiovascular research. 2009; 84(3):485–93. [PubMed: 19592568]
14. Murao K, Ohyama T, Imachi H, Ishida T, Cao WM, Namihira H, Sato M, Wong NC, Takahara J. TNF-alpha stimulation of MCP-1 expression is mediated by the Akt/PKB signal transduction pathway in vascular endothelial cells. Biochem Biophys Res Commun. 2000; 276(2):791–6. [PubMed: 11027549]
15. Videm V, Albrigtsen M. Soluble ICAM-1 and VCAM-1 as markers of endothelial activation. Scand J Immunol. 2008; 67(5):523–31. [PubMed: 18363595]
16. Yoshida T, Yamashita M, Horimai C, Hayashi M. Deletion of Kruppel-like factor 4 in endothelial and hematopoietic cells enhances neointimal formation following vascular injury. J Am Heart Assoc. 2014; 3(1):e000622. [PubMed: 24470523]
17. Huang H, Jing G, Wang JJ, Sheibani N, Zhang SX. ATF4 is a novel regulator of MCP-1 in microvascular endothelial cells. J Inflamm (Lond). 2015; 12:31. [PubMed: 25914608]

18. Hutter R, Carrick FE, Valdiviezo C, Wolinsky C, Rudge JS, Wiegand SJ, Fuster V, Badimon JJ, Sauter BV. Vascular endothelial growth factor regulates reendothelialization and neointima formation in a mouse model of arterial injury. Circulation. 2004; 110(16):2430–5. [PubMed: 15477421]

19. Forstermann U, Munzel T. Endothelial nitric oxide synthase in vascular disease: from marvel to menace. Circulation. 2006; 113(13):1708–14. [PubMed: 16585403]

20. Pham PT, Pham PC, Danovitch GM, Ross DJ, Gritsch HA, Kendrick EA, Singer J, Shah T, Wilkinson AH. Sirolimus-associated pulmonary toxicity. Transplantation. 2004; 77(8):1215–20. [PubMed: 15114088]

21. Fang Y, Westbrook R, Hill C, Boparai RK, Arum O, Spong A, Wang F, Javors MA, Chen J, Sun LY, Bartke A. Duration of rapamycin treatment has differential effects on metabolism in mice. Cell Metab. 2013; 17(3):456–62. [PubMed: 23473038]

22. Lu Z, Liu F, Chen L, Zhang H, Ding Y, Liu J, Wong M, Zeng LH. Effect of Chronic Administration of Low Dose Rapamycin on Development and Immunity in Young Rats. PloS one. 2015; 10(8):e0135256. [PubMed: 26248290]

23. Huang M, Qiu Q, Xiao Y, Zeng S, Zhan M, Shi M, Zou Y, Ye Y, Liang L, Yang X, Xu H. BET Bromodomain Suppression Inhibits VEGF-induced Angiogenesis and Vascular Permeability by Blocking VEGFR2-mediated Activation of PAK1 and eNOS. Scientific reports. 2016; 6:23770. [PubMed: 27044328]

24. Balcells M, Martorell J, Olive C, Santacana M, Chitalia V, Cardoso AA, Edelman ER. Smooth muscle cells orchestrate the endothelial cell response to flow and injury. Circulation. 2010; 121(20):2192–9. [PubMed: 20458015]

25. Sheikhpour M, Barani L, Kasaeian A. Biomimetics in drug delivery systems: A critical review. Journal of controlled release: official journal of the Controlled Release Society. 2017; 253:97–109. [PubMed: 28322976]

26. Jung SM, Moroi M. Platelet glycoprotein VI. Advances in experimental medicine and biology. 2008; 640:53–63. [PubMed: 19065783]

27. Asangani IA, Dommeti VL, Wang X, Malik R, Cieslik M, Yang R, Escara-Wilke J, Wilder-Romans K, Dhanireddy S, Engelke C, Iyer MK, Jing X, Wu YM, Cao X, Qin ZS, Wang S, Feng FY, Chinnaiyan AM. Therapeutic targeting of BET bromodomain proteins in castration-resistant prostate cancer. Nature. 2014; 510(7504):278–82. [PubMed: 24759320]

28. Korb E, Herre M, Zucker-Scharff I, Darnell RB, Allis CD. BET protein Brd4 activates transcription in neurons and BET inhibitor Jq1 blocks memory in mice. Nature neuroscience. 2015; 18(10): 1464–73. [PubMed: 26301327]

29. Niu N, Shao R, Yan G, Zou W. Bromodomain and Extra-terminal (BET) Protein Inhibitors Suppress Chondrocyte Differentiation and Restrain Bone Growth. The Journal of biological chemistry. 2016; 291(52):26647–26657. [PubMed: 27821592]

30. Augustin HG, Koh GY. Organotypic vasculature: From descriptive heterogeneity to functional pathophysiology. Science. 2017

Highlights

- The standard of care for atherosclerosis and restenosis (vessel re-narrowing) is balloon angioplasty followed by the implantation of a drug-eluting stent; an inherent problem is endothelial damage and associated thrombotic risks imposed by current drugs and stenting.
- We created a preclinical anti-restenotic system that incorporates the combined merits of an epigenetic modulator, its nanocarrier and their coating with a biomimetic membrane.
- This biomimetic system is intravenously injectable (stent-free) and can home to the injured arterial wall thereby attenuating post-angioplasty restenosis. Of particular significance, it also circumvents the impairment of endothelial recovery that occurs with the status-quo drug rapamycin.
- This system may confer an adjustability of therapeutic regimen (i.e., drugs, doses, and injection timing and frequency) and amenability toward combination therapy and precision medicine.

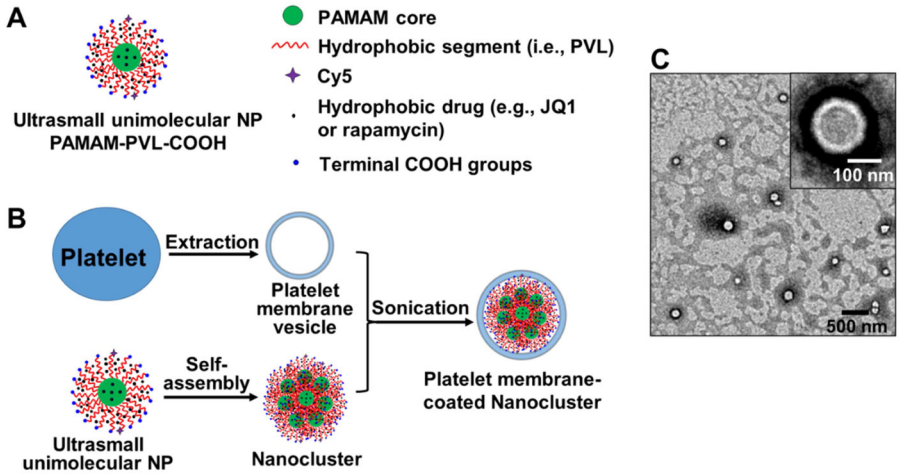

Figure 1. Schematic preparation and characterization of biomimetic nanoclusters

A. Schematic illustration of a drug-loaded PAMAM-PVL ultrasmall unimolecular NP. B. Illustration for the preparation of a platelet membrane-coated nanocluster. C. TEM image of platelet membrane-coated nanoclusters. The inset shows an enlarged image of a single biomimetic nanocluster.

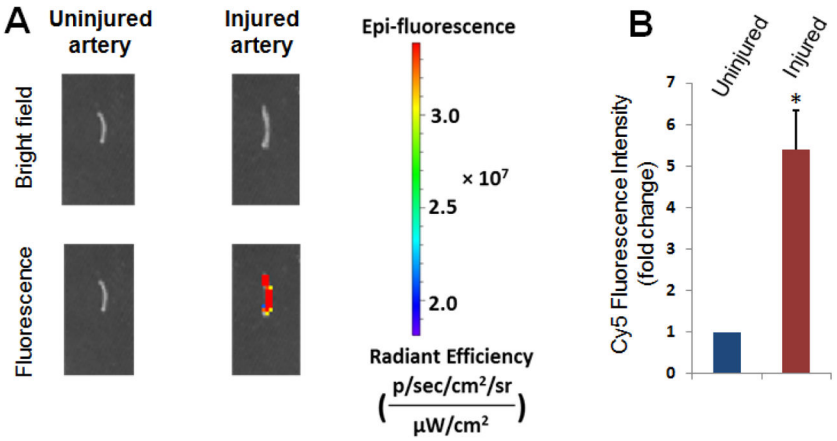

Figure 2. Homing of biomimetic nanoclusters to injured carotid arteries

Cy5-tagged nanoclusters were coated with platelet membranes, as described in Figure 1, and tail-vein injected (2.5 mg/kg animal weight) immediately after balloon angioplasty of the rat carotid artery. A. Balloon-Injured arteries and uninjured contralateral arteries were collected 5 days later for ex vivo imaging with an IVIS spectrum luminescence system (Ex/Em: 650/720 nm). More images from other 5 rats were presented in Figure S2. B. Quantification: Mean ± SEM, n=6 rats; *$p<0.05$. The intensity of basal level fluorescence from uninjured control (presented as 1) was used for normalization of the fluorescence in injured arteries.

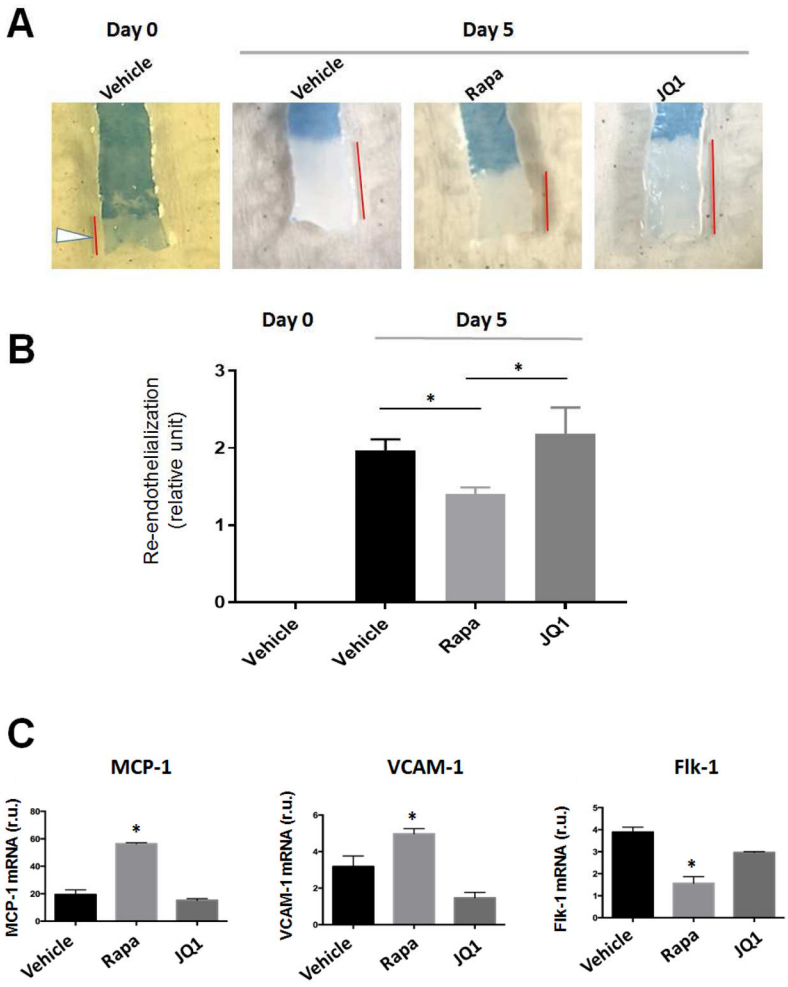

Figure 3. Effects of drug-loaded biomimetic nanoclusters on re-endothelialization in balloon-injured arteries

Injections of biomimetic nanoclusters were performed as described in the Methods section. Animals were euthanized at 5 days post-angioplasty. Carotid arteries were collected and stained with Evans Blue.

A. Representative images of Evans Blue staining of carotid arteries. Denuded areas were stained blue; the unstained artery length is indicated by a red bar. Day-0 arteries were stained immediately after balloon angioplasty injury, thus there was no re-endothelialization at this time point.

B. Quantification of re-endothelialization. In every rat carotid artery, balloon angioplasty commonly left the proximal end uninjured (see arrowhead in A, Day-0). The length of this uninjured segment was therefore used as a common denominator to normalize unstained artery lengths in all conditions. Re-endothelialization was then calculated by subtracting the normalized value of the Day-0 condition in which no re-endothelialization occurred. Mean ± SEM, n=3 rats; *$p<0.05$.

C. Analysis of endothelial cell markers. Evans Blue-stained arteries were transiently fixed with RNAlater solution and subjected to RNA extraction and qPCR analysis. Quantification: Mean ± SEM, n=3 rats; *$p<0.05$ compared to vehicle control.

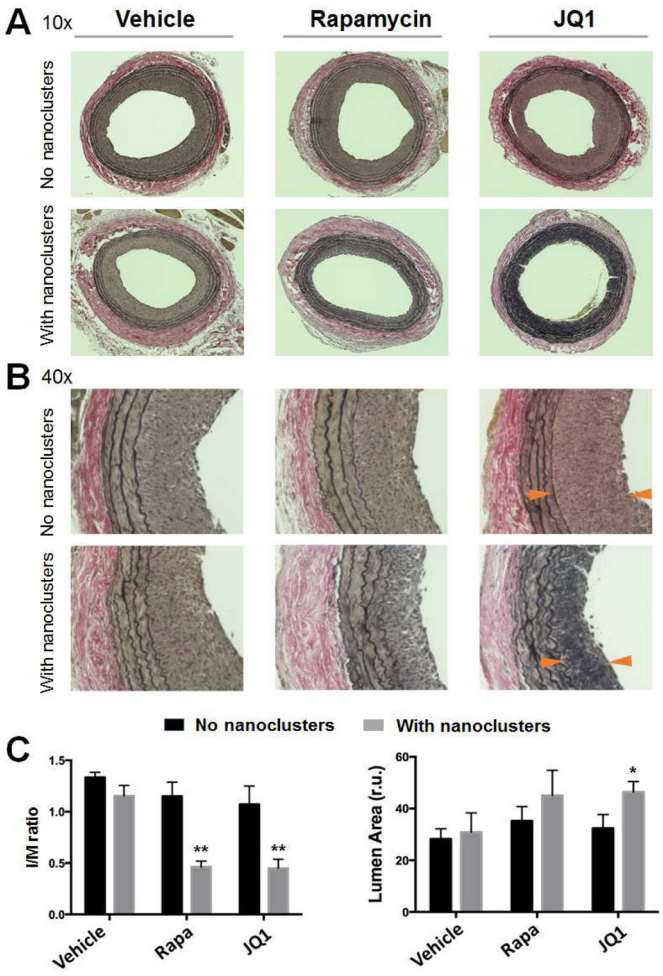

Figure 4. Anti-restenotic effects of drug-loaded biomimetic nanoclusters in balloon-injured arteries

Rapamycin- or JQ1-loaded biomimetic nanoclusters, or their respective drug-only controls (no nanoclusters) were injected into the rat tail vein right after the carotid artery angioplasty. The injection was repeated 4 days later. Injected additional controls included PBS (no drug, no nanoclusters) and empty biomimetic nanoclusters (no drug). Animals were euthanized at 14 days post-angioplasty. Arteries were collected, and their cross-sections were prepared and Verhoeff-van Gieson (VvG)-stained for morphometric analysis. Neointimal hyperplasia (IH) was measured by the intimal/medial area ratio (I/M ratio); anti-restenotic effect was reflected by an increase (versus vehicle) of the lumen area. A. Representative images (10×) of VvG-stained artery sections. B. 40X images. C. Quantification of I/M ratios and lumen areas. One-way ANOVA followed by Bonferroni post-hoc analysis was performed. Mean ± SEM, n= 6–8 rats. **P<0.01 compared to any other condition except between Rapa and JQ1; *P<0.05 compared to the vehicle control (no nanoclusters); otherwise no significance was detected.